Nuclear cysteine cathepsin variants in thyroid carcinoma cells

Sofia Tedelind[1,*], Kseniia Poliakova[1], Amanda Valeta[1], Ruth Hunegnaw[1], Eyoel Lemma Yemanaberhan[1], Nils-Erik Heldin[2], Junichi Kurebayashi[3], Ekkehard Weber[4], Nataša Kopitar-Jerala[5], Boris Turk[5], Matthew Bogyo[6] and Klaudia Brix[1]

[1] School of Engineering and Science, Research Center of Molecular Life Science, Jacobs University Bremen, Campus Ring 1, D-28759 Bremen, Germany
[2] Department of Genetics and Pathology, Uppsala University, S-75185 Uppsala, Sweden
[3] Department of Breast and Thyroid Surgery, Kawasaki Medical School, 701-0192 Okayama, Japan
[4] Institute of Physiological Chemistry, Martin Luther University, D-06097 Halle-Wittenberg, Germany
[5] Department of Biochemistry, Molecular and Structural Biology, Jožef Stefan Institute, SI-1000 Ljubljana, Slovenia
[6] Departments of Pathology and Microbiology and Immunology, Stanford University School of Medicine, 300 Pasteur Dr., Stanford, CA 94305-5324, USA

* Corresponding author
  e-mail: s.tedelind@jacobs-university.de

Abstract

The cysteine peptidase cathepsin B is important in thyroid physiology by being involved in thyroid prohormone processing initiated in the follicular lumen and completed in endo-lysosomal compartments. However, cathepsin B has also been localized to the extrafollicular space and is therefore suggested to promote invasiveness and metastasis in thyroid carcinomas through, e.g., ECM degradation. In this study, immunofluorescence and biochemical data from subcellular fractionation revealed that cathepsin B, in its single- and two-chain forms, is localized to endo-lysosomes in the papillary thyroid carcinoma cell line KTC-1 and in the anaplastic thyroid carcinoma cell lines HTh7 and HTh74. This distribution is not affected by thyroid stimulating hormone (TSH) incubation of HTh74, the only cell line that expresses a functional TSH-receptor. Immunofluorescence data disclosed an additional nuclear localization of cathepsin B immunoreactivity. This was supported by biochemical data showing a proteolytically active variant slightly smaller than the cathepsin B proform in nuclear fractions. We also demonstrate that immunoreactions specific for cathepsin V, but not cathepsin L, are localized to the nucleus in HTh74 in peri-nucleolar patterns. As deduced from co-localization studies and *in vitro* degradation assays, we suggest that nuclear variants of cathepsins are involved in the development of thyroid malignancies through modification of DNA-associated proteins.

Keywords: cysteine peptidases; HTh7; HTh74; KTC-1; nuclear proteases.

Introduction

Related members of cysteine cathepsins exhibit a broad variety in terms of tissue expression and function (Reinheckel et al., 2001; Turk et al., 2001; Brix et al., 2008). Some of these peptidases are ubiquitously expressed, others are specific to a tissue or cell-type. Cysteine cathepsins are co-translationally targeted to the endoplasmic reticulum (ER) through the N-terminal signal peptide and further trafficked as a proprotein with destination to endo-lysosomes (Linke et al., 2002a; Brix, 2005). In the acidic milieu of endo-lysosomes, cathepsins obtain their mature form through proteolytic removal of the pro-peptides followed by exposure of the active site (Mach et al., 1994; Turk et al., 2000). Cysteine cathepsins are also proteolytically active in the extracellular space despite an 'unfavorable' milieu with a neutral pH and oxidizing conditions (Brix et al., 1996, 2001; Buth et al., 2007; Jordans et al., 2009). Cysteine cathepsin functions are numerous and are determined, in part, by their location; bulk degradation of proteins and participation in antigen presentation in endo-lysosomes, or extracellular matrix (ECM) remodeling in wound healing (Riese and Chapman, 2000; Turk et al., 2001; Friedrichs et al., 2003; Buth et al., 2007). Importantly, the thyroid epithelium is one of few locations where a tissue specific natural substrate of cysteine cathepsins has been identified. The prohormone thyroglobulin (Tg) is initially processed for thyroid hormone liberation in the extracellular thyroid follicle lumen followed by endo-lysosomal cleavage mediated by cathepsins B, K and L (Brix et al., 1996; Friedrichs et al., 2003). The cathepsins thus encounter their natural substrate in several different compartments within a thyrocyte to which they have to be correctly targeted. Endo-lysosomal targeting is believed to be mediated via a mannose 6-phosphate tag and the corresponding receptors in the trans-Golgi-network (TGN) (Ludwig et al., 1994) whereas the secretion of mature cathepsin B into the follicular lumen is a regulated process stimulated by TSH, the thyroid stimulating hormone (Linke et al., 2002b).

Newly discovered cathepsin functions are continuously being added to an already impressive list, also owing to the increasing number of studies demonstrating nuclear localization of these cysteine peptidases. For example, MENT, a serpin that interacts with chromatin for its condensation, has been localized to the nucleus and was shown to be a strong

inhibitor of cathepsin V, but not L, in DNA-rich environments (Ong et al., 2007). Therefore, this was an indication of a function of a cysteine cathepsin if it localized to the nucleus of mammalian cells. Furthermore, it was shown before that the interaction of MENT with a nuclear papain-like cysteine proteinase caused a block in proliferation (Irving et al., 2002). However, it was also demonstrated that nuclear cathepsin L can promote cell cycle progression through CUX1 transcription factor cleavage (Goulet et al., 2004). Recently, a role of nuclear cathepsin L was suggested to even take part in mouse embryonic stem cell differentiation (Duncan et al., 2008).

Cysteine cathepsins have long been suggested to be involved in malignancies and cancer progression owing to an increase in expression and activity in cancer cells and tumor-associated tissue (Sloane and Honn, 1984; Joyce et al., 2004; Turk et al., 2004; Gocheva et al., 2006). Thyroid cathepsin, e.g., has been shown to be localized to the basement membrane of thyroid carcinoma cells *in situ*, which might facilitate tumor invasiveness and metastasis through degradation of the extracellular matrix (Shuja and Murnane, 1996). Moreover, an increased expression and activity of nuclear cathepsin L in transformed mouse cells (Goulet et al., 2007) and colorectal carcinoma cells (Sullivan et al., 2009) is taken as an indication of the role of nuclear cysteine cathepsin variants in cancer development and progression through yet to be uncovered molecular mechanisms. Hence, we propose that cysteine cathepsins in thyroid carcinoma can promote cancer progression by other means than paving the way for migrating cells through the extracellular matrix. In this study we therefore analyzed the subcellular location of cysteine cathepsins in the thyroid carcinoma cell lines KTC-1, HTh7 and HTh74 that serve as models for poorly differentiated papillary and anaplastic thyroid carcinomas. We show that proteolytically active variants of cysteine cathepsins B and V are localized to the cell nucleus and suggest that an interaction with DNA-associated proteins and with other nuclear proteins could play a role in the development of thyroid malignancies.

Results

HTh74 expresses TSH-receptor mRNA and responds to TSH stimulation

The poorly differentiated papillary carcinoma cell line KTC-1 and the anaplastic thyroid carcinoma cell lines HTh7 and HTh74 have been shown to express low levels of thyroid-specific genes such as sodium iodide symporter (NIS), thyroperoxidase (TPO) and Tg (Heldin and Westermark, 1991). Only HTh74 is believed to possess a functional TSH-receptor (TSH-R) which we confirmed by RT-PCR amplification of its mRNA (Figure 1A). Upon stimulation of HTh74 cultures with 100 μU/ml TSH for 48 h, the amount of TSH-receptor mRNA decreased (Figure 1B), highlighting down-regulation of the receptor under conditions of chronic TSH stimulation as expected from its negative feedback regulation
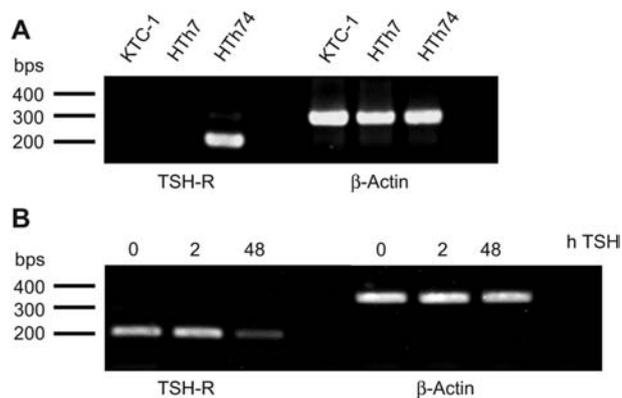

Figure 1 Expression of TSH-receptor mRNA in thyroid carcinoma cells.
(A) RT-PCR amplification of TSH-receptor and β-actin mRNA in KTC-1, HTh7 and HTh74 cells as analyzed by agarose gel electrophoresis. (B) TSH-receptor mRNA levels in HTh74 cells stimulated with 100 μU/ml TSH for the indicated time intervals. Amplicons were analyzed by agarose gel electrophoresis and amplification of β-actin mRNA was used as a loading control.

in vivo. The results demonstrated that the HTh74 cell line can thus serve as a model for TSH-responsive thyroid carcinoma cells.

Cathepsin B variants in thyroid carcinoma cells

Previously, we have shown that cathepsin B is secreted from primary pig thyrocytes upon short-term TSH stimulation, whereas stimulation with TSH over several hours resulted in up-regulation of its *de novo* biosynthesis (Linke et al., 2002b). Therefore, we thought to analyze synthesis of cathepsin B and its molecular forms in thyroid carcinoma before and after short-term stimulation with TSH. Immunoblotting of cathepsin B in lysates of KTC-1, HTh7 and HTh74 cells demonstrated the expected molecular forms of the protease, i.e., the proform, single-chain, and the heavy chain of the two-chain form (Figure 2A,C,E; left panels). In all three cell lines the major proportion of cathepsin B was the heavy chain which constituted approximately 50% of the total immunoreactivity. The single-chain form constituted 20–40%, whereas the proform amounted to only approximately 20% or less in lysates prepared from non-stimulated cells (Figure 2B,D,F). It is of note that these ratios were highly reproducible and remained largely unaltered upon TSH stimulation for up to 4 h. Interestingly, a 40-kDa variant of cathepsin B was detected in all cell lines (Figure 2, arrowheads in right margins) that constituted approximately 5–15% of the total cathepsin B content in KTC-1, HTh7 and HTh74 (Figure 2B,D,F). We reasoned that such variants might either represent unusual processing intermediates of cathepsin B in thyroid carcinoma, or alternatively, that the variants represented an N-terminally truncated form of cathepsin B lacking the signal peptide. The latter hypothesis is supported by the notion of multiple transcription start sites
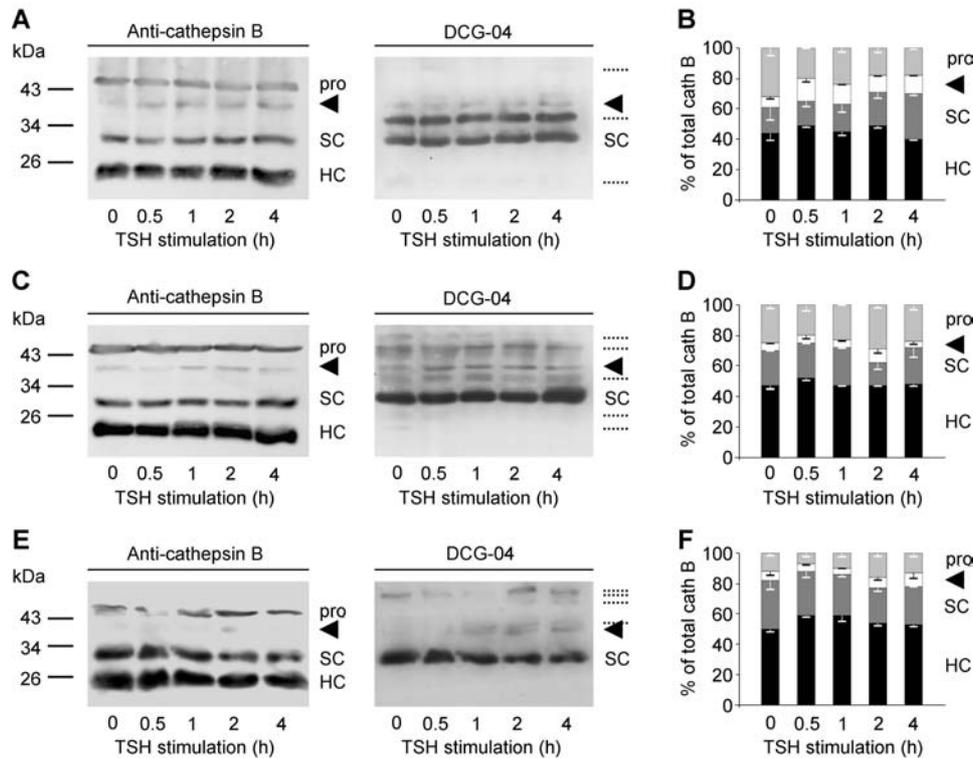
Figure 2 Protein levels of cathepsin B and active cysteine peptidases in thyroid carcinoma cells.
Immunoblots (anti-cathepsin B), streptavidin reacted blots (DCG-04) and densitometry analysis of the molecular forms of cathepsin B (left panels of A,C,E) and active cysteine peptidases (right panels of A,C,E) present in cell lysates of KTC-1 (A,B), HTh7 (C,D), and HTh74 cells (E,F) at the indicated time intervals after stimulation with 100 μU/ml TSH. The expected molecular forms of cathepsin B were detected in all cell lines, i.e., proform (pro), single-chain form (SC) and the heavy chain (HC) of the two-chain form. In addition, a protein band with an apparent molecular mass of approximately 40 kDa (arrowheads) was detected in the lysates of all three cell lines. The single chain and the 40 kDa forms of cathepsin B were shown to be active through detection of the biotinylated activity based probe DCG-04 that binds to active cysteine peptidases in a 1:1 ratio. Active non-cathepsin B peptidases are indicated with dashed lines in the right margins of A,C,E. Molecular mass markers are indicated in the left margins of A,C,E. Proteins were separated by SDS-PAGE, immunoblotted with goat anti-mouse cathepsin B or peroxidase-conjugated streptavidin and visualized through enhanced chemiluminescence. Densitometry analysis of all bands recognized by anti-cathepsin B antibodies revealed the stoichiometry of the various molecular forms in KTC-1 (B), HTh7 (D) and HTh74 cells (F) with total immunodetected cathepsin B set to 100%. Light gray, dark gray and black bars denote the proform, single and heavy chain forms of cathepsin B, whereas the 40 kDa form is represented by white boxes. Values are given as means-SD.

in the human cathepsin B gene detected in, e.g., gastric adenocarcinoma, and breast and colon carcinoma (Gong et al., 1993; Berquin et al., 1995).

To gain information about the proteolytically active forms of cysteine peptidases in the thyroid carcinoma cell lines, lysates were prepared in the presence of the activity based probe DCG-04. This probe binds to active forms of cysteine cathepsins in a 1:1 ratio and bears a biotin tag (Greenbaum et al., 2000; Fonovic and Bogyo, 2008). By incubating the membranes with peroxidase-conjugated streptavidin, it was shown that the active site in the single-chain of cathepsin B was tagged as expected in all cell lines (Figure 2A,C,E, right panels, SC). Likewise, the light chains containing the active-site cysteine of two-chain cathepsin B were labeled also (not shown). In addition, the truncated variants of cathepsin B in the analyzed cell lines were also shown to be active because a 40-kDa band appeared when visualizing the complexes of DCG-04 and its target cysteine peptidases (Figure 2A,C,E, right panels, arrowheads). Of specific note is that the protein

levels of the active cathepsin B variant increased upon TSH stimulation of HTh74 for 1–4 h (Figure 2E, right panel, arrowhead). This finding of short-term TSH-induced up-regulation of the 40-kDa variant in HTh74 cells prompted us to focus on this cell line for the further studies.

The number of active cysteine cathepsins that are not represented by cathepsin B varied greatly between the different cell lines (Figure 2A,C,E, right panels, dashed lines). KTC-1 displayed one major and two minor active cysteine peptidases (Figure 2A), whereas HTh7 and HTh74 whole cell lysates featured only several minor active cysteine peptidases that were not cathepsin B (Figure 2C,E, respectively). Hence, in HTh74 cells cathepsin B was the most prominent cysteine peptidase present, and the results thus motivated us to analyze its subcellular localization in detail (see below). The variation in the number of active cysteine cathepsins between the different cell lines might be relevant for their malignant characteristics. This is, however, not within the scope of this study but will require further detailed analysis.

Cathepsin B is visualized in the nuclei of proliferating thyroid carcinoma cell lines by immunofluorescence

Visualization of cathepsin B through indirect immunofluorescence displayed the expected vesicular staining pattern in all three cell lines (Figure 3A,C,E,G). The vesicles were scattered throughout the cytosol in KTC-1 cells (Figure 3A), whereas they accumulated in the perinuclear region and often in the dent of the kidney-shaped nuclei of HTh7 and HTh74
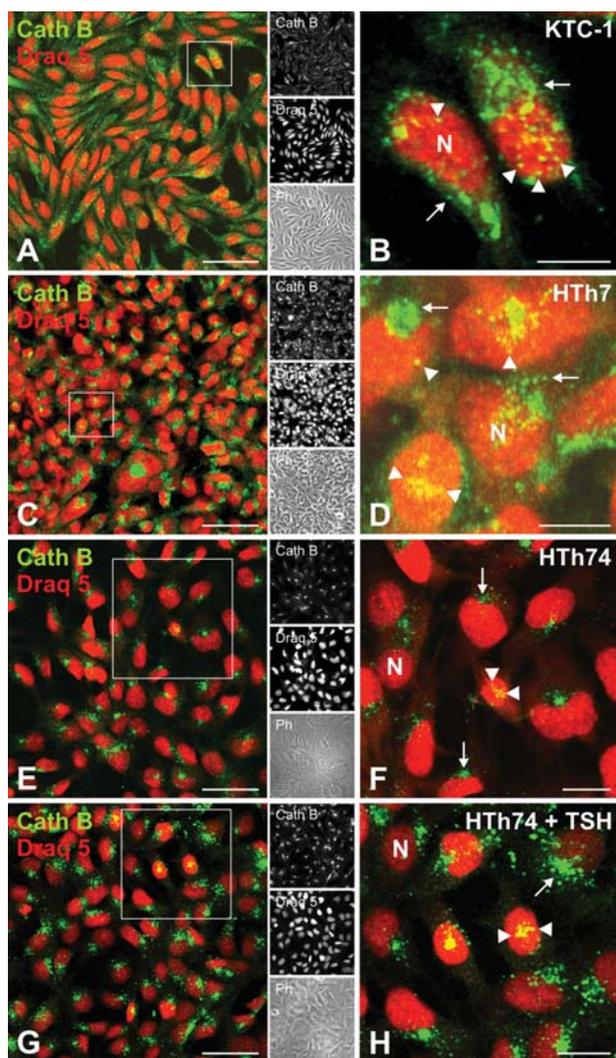

Figure 3 Localization of cathepsin B in thyroid carcinoma cells. Single channel fluorescence (right panels, top and middle), merged (A–H) and corresponding phase contrast micrographs (right panels, bottom) of KTC-1 (A), HTh7 (C) and HTh74 cells (E,G). Boxed areas in A,C,E,G are magnified in B,D,F,H, respectively. Cells were immunolabeled after PFA fixation and Triton X-100 permeabilization with cathepsin B-specific antibodies (green signals; right panels, top) and nuclei were counter-stained with DRAQ5™ (red signals; right panels, middle). Cathepsin B was mainly localized to vesicles scattered throughout the cytosol and accumulating in the peri-nuclear regions of thyroid carcinoma cells (arrows). Note that cathepsin B was additionally located in the nuclei (arrowheads). Scale bars correspond to 50 μm in A,C,E,G, 20 μm in F,H, and 10 μm in B,D. N denotes nuclei.

cells (Figure 3C,E, respectively). Higher magnifications revealed that cathepsin B immunoreactivity was also localized to the nuclei of all three cell lines, which was particularly obvious in cells that were eventually fixed at the end of M-phase (Figure 3B,D,F, arrowheads). Similarly, TSH-stimulated HTh74 cells also displayed a nuclear localization of cathepsin B which was confined to one patchy region within the nuclei (Figure 3G,H, arrowheads).

The nuclear fraction of HTh74 contains a truncated cathepsin B variant

To further determine the molecular forms of cathepsin B in different compartments of thyroid carcinoma cells, immunoblotting of cathepsin B was performed with subcellular fractions purified from HTh74 cells before and after TSH stimulation. The whole cell fraction contained the expected molecular forms of cathepsin B, i.e., the proform, the single-chain and the heavy chain of two-chain cathepsin B (Figure 4A). In addition, a variant with an apparent molecular mass of 40 kDa was detected in whole cell lysates and in the nuclear fractions, but remarkably not in lysosomal and plasma membrane fractions (Figure 4A, arrowhead), indicating that this cathepsin B variant indeed represents a nuclear form of the protease. Because this molecular form was not detectable in lysosomes or at the plasma membrane, we conclude that it indeed lacks the signal peptide which co-translationally targets procathepsin B for ER-entry. Hence, the nuclear cathepsin B variant is likely to be N-terminally truncated (Figure 4D).

Purity of the subcellular fractions was assessed by immunoblotting of resident proteins used as markers. As expected for thyrocytes (Lemansky et al., 1998), the intermediate form and the heavy chain of cathepsin D with molecular masses of approximately 41 and 31 kDa were enriched in the lysosomal fractions but absent from the nuclei (Figure 4B). High mobility group box 1 protein (HMGB1) was detected in whole cell lysates and nuclear fractions as expected for this DNA-binding protein (Figure 4C). Note that neither of these nuclear or endo-lysosomal proteins was detected in the plasma membrane fractions. Furthermore, TSH stimulation did not affect the expression of the nuclear variant of cathepsin B or its subcellular localization (Figure 4A). This latter result is in accordance with the observation that TSH-stimulated up-regulation of the 40-kDa variant is only in the range of approximately 5% of the total cathepsin B (compare Figure 2F, white bars, arrowhead).

In vitro degradation of nuclear proteins by cathepsin B

Nuclear variants of cysteine cathepsins have been suggested to change the epigenetic landscape or process transcription factors and DNA-associated proteins such as histone H3 (Bulynko et al., 2006; Goulet et al., 2006; Duncan et al., 2008) which might play a role in regulation of cell differentiation and proliferation. We have shown that the nuclear 40-kDa truncated variants of cathepsin B in thyroid carcinoma cell lines are active (see above), and to get an initial
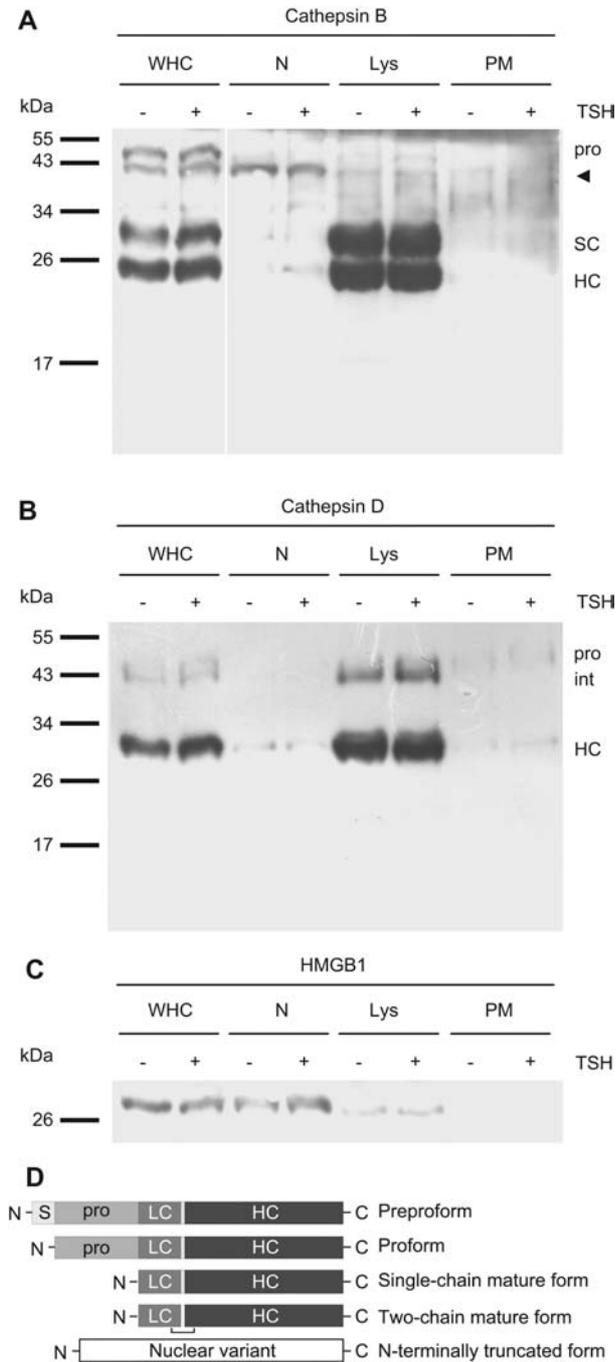
Figure 4 Cathepsin B variant in the nucleus of HTh74 cells. Immunoblots of cathepsin B (A), cathepsin D (B), and HMGB1 (C) of lysates prepared from whole cells (WHC), nuclear (N), lysosomal (Lys) or plasma membrane (PM) fractions of non-stimulated controls (-) and HTh74 cells stimulated with 100 μU/ml TSH for 4 h (+). The expected molecular forms of cathepsin B were detected in whole cell lysates and lysosomal fractions but not in nuclear fractions (A), i.e., proform (pro), single-chain form (SC), and the heavy chain (HC) of the two-chain form. An enrichment of mature cathepsin B was observed in the lysosomal fractions as expected (A; SC and HC). In addition, a 40-kDa band was the only band detected in nuclear fractions (A; arrowhead) and, hence, probably represented an N-terminally truncated variant of cathepsin B. Cathepsin D (B) and HMGB1 (C) were used as markers for the purity of lysosomal and nuclear fractions, respectively. Note the enrichment of the intermediate form (int) and of the heavy chain (HC) of cathepsin D but not of the proform (pro) in lysosomal fractions as expected (B). Molecular mass markers are indicated in the left margins of A–C. Proteins were separated by SDS-PAGE and immunoblotted with goat anti-mouse cathepsin B, mouse anti-human cathepsin D and rabbit anti-human HMGB1 antibodies, and visualized through enhanced chemiluminescence. (D) Schematic illustration of the molecular forms of cathepsin B and its nuclear variant. S denotes signal peptide, pro indicates the immature zymogene form of the enzyme, HC and LC denote heavy and light chains of mature cathepsin B, respectively.

ence of cathepsin B (Figure 5A, lanes 4 and 6, open arrowhead; Figure 5B), whereas several proteins with lower molecular masses appeared after 1 and 4 h of incubation (Figure 5A, lanes 4 and 6, arrow; Figure 5D). The results indicated that cathepsin B variants with cysteine peptidase activity can, in principle, cleave nuclear targets. Moreover, cleavage of nuclear proteins by cathepsin B-like peptidases is likely to be specific rather than general as might be anticipated from the broad substrate specificity of cathepsin B, because a general degradation of nuclear fraction proteins was not observed as a result of cathepsin B incubation.

To identify some possible nuclear substrates of cathepsin B variants, we probed immunoblots of SDS-PAGE separated nuclear fraction proteins of HTh74 cells before and after incubation with cathepsin B for 4 h with antibodies specific for histone H1 and HMGB1, both being abundantly present within the nucleus. A band at approximately 35 kDa was recognized by an anti-histone H1 antibody and it disappeared upon incubation of nuclear fractions with cathepsin B (Figure 5F). In sharp contrast, HMGB1 with a molecular mass of approximately 27 kDa remained unaltered (Figure 5E), supporting the notion that cleavage mediated by cathepsin B variants is likely to be specific and involved in a confined change of the landscape of DNA-associated proteins within the nucleus of human thyroid carcinoma cells.

Cathepsin L and V variants in thyroid carcinoma cells

As deduced from the results in Figure 2, the thyroid carcinoma cell lines contained numerous proteolytically active cysteine peptidases that are not cathepsin B. To elucidate the nature of these non-cathepsin B bands, lysates from HTh74 cells were analyzed with respect to their content of other

idea of a possible function in this new compartment, we incubated nuclear fractions isolated from HTh74 cells with cathepsin B for 0, 1 and 4 h. Nuclear fraction proteins with or without cathepsin B addition were separated through sodium dodecyl sulfate polyacrylamide gel electrophoresis (SDS-PAGE) and visualized through silver staining. The majority of proteins in the nuclear fractions of HTh74 cells have a molecular mass of above 30 kDa (Figure 5A, lanes 1–6). The lanes containing proteins with molecular masses ≤30 kDa represented nuclear fractions that were incubated with cathepsin B (Figure 5A, lanes 2, 4 and 6). In addition, several high molecular mass proteins disappeared in the pres-
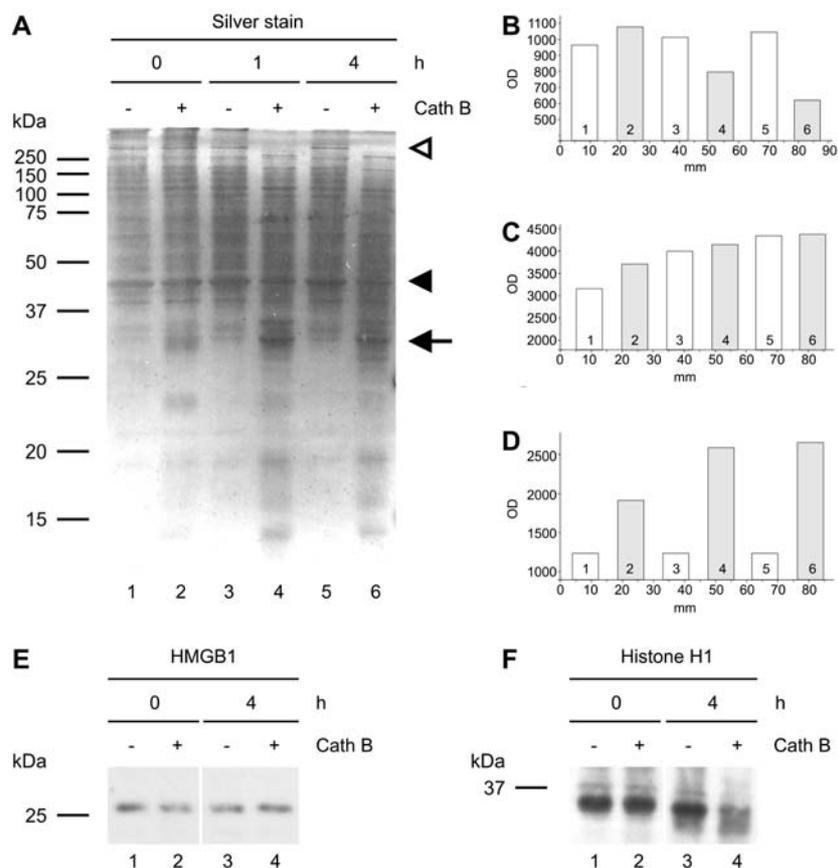
Figure 5   Degradation of nuclear proteins by cathepsin B.

Visualization of proteins in nuclear fractions prepared from HTh74 cells was through SDS-PAGE and silver staining before (-) and after (+) incubation with cathepsin B at 37°C for the indicated time intervals. Incubation with cathepsin B (lanes 2, 4 and 6 in A) resulted in disappearance of protein bands (compare lanes 4 and 6 with lane 2 in A, open arrowhead, and gray bars in B) or appearance of protein bands (compare lanes 4 and 6 with lane 2 in A, arrow, and gray bars in D), whereas most proteins of nuclear fractions remained unaffected (compare lanes 1–6 in A, closed arrowhead, and gray bars in C). Densitometry analysis of representative bands (B–D) was performed to determine optical densities (OD) along a profile line across lanes 1 through 6 positioned as indicated in A by open and closed arrowheads and arrow, respectively. Mean intensities of the bands are given in the bar charts in B–D, white and gray bars represent nuclear fractions without and with cathepsin B incubation, respectively. Immunoblots of nuclear fractions prepared from HTh74 cells before and after incubation with cathepsin B at 37°C for 0 and 4 h were probed with anti-HMGB1 (E) and anti-histone H1 (F) antibodies. Whereas HMGB1 was not affected by cathepsin B incubation (E), linker histone H1 was degraded within 4 h and processed to two faster migrating bands (F). Molecular mass markers are indicated in the left margins. Proteins were separated by SDS-PAGE and immunoblotted with specific antibodies and secondary, peroxidase-coupled antibodies before visualization through enhanced chemiluminescence.

cysteine peptidases. Moreover, we recently detected nuclear cathepsin L variants spontaneously expressed in a rat intestine epithelial cell line (Brix et al., 2008; Mayer et al., 2009), and were therefore interested to learn whether nuclear cathepsin L localization is also typical for such human cell lines that sort an N-terminally truncated variant of cathepsin B to their nuclear compartment. In the cell lysates of HTh74 cells, all expected forms of cathepsin L were detected (Figure 6A). Furthermore, it was shown that the highest protein level of cathepsin L was in endo-lysosomal compartments but it was completely absent from the nuclei as determined by subcellular fractionation (Figure 6B). Because the human genome codes for cathepsin V, the closest relative of cathepsin L, we further investigated whether cathepsin V might localize to the nucleus instead. Cathepsin V was shown to be present in the nuclear fraction as a 40-kDa molecular mass protein (Figure 6C, arrowhead) whereas its glycosylated and

non-glycosylated mature forms (Bromme et al., 1999) were detected in the lysosomal fraction (Figure 6C). The non-glycosylated form of cathepsin V was more prominent in the lysosomal fraction than the glycosylated form. Similar to cathepsins B and L, the protein levels of the cathepsin V forms remained unchanged in response to TSH stimulation (Figure 6D). By identifying active cysteine cathepsins with the activity based probe DCG-04, we determined that the glycosylated form of cathepsin V and importantly, the 40-kDa cathepsin V form enriched in nuclear fractions were proteolytically active (Figure 6E).

Cathepsin V but not L is localized to the nucleus of HTh74 cells

As mentioned above, several recent studies have shown the localization of cysteine cathepsins in the nucleus of various
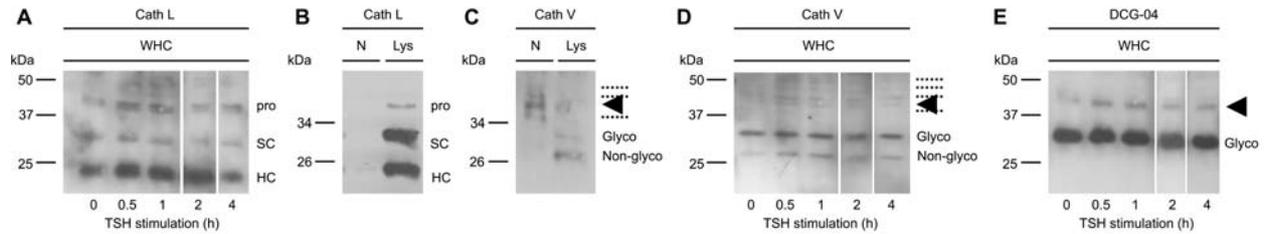
Figure 6 Active cathepsin V variant in the nucleus of HTh74 cells.
Immunoblots of cathepsin L (A,B) and cathepsin V (C,D) in lysates prepared from whole cells (WHC), nuclear (N) or lysosomal (Lys) fractions of TSH (100 μU/ml) stimulated HTh74 cells. The expected molecular forms of cathepsin L, i.e., proform (pro), single-chain form (SC), and the heavy chain (HC) of the two-chain form were detected in the whole cell lysate (A), mature forms were enriched in the lysosomal fraction (B, Lys, SC, HC) but none of the forms was detected in the nuclear fraction of HTh74 cells (B, N). By contrast, a cathepsin V variant of approximately 40 kDa was present exclusively in nuclear but not in the lysosomal fraction of HTh74 cells (C, arrowhead) in which cathepsin V was immunodetected primarily in its non-glycosylated form (C, non-glyco cf. glyco). Active cysteine peptidases were visualized in the identical samples immunoblotted in D through streptavidin detection of the biotinylated activity based probe DCG-04 that was added during lysate preparation and binds to active cysteine peptidases in a 1:1 ratio (E). The glycosylated and the 40 kDa forms of cathepsin V were shown to be proteolytically active (E, glyco and arrowhead). Molecular mass markers are indicated in the left margins. Proteins were separated by SDS-PAGE and immunoblotted with mouse anti-human cathepsin L (A,B) and mouse anti-human cathepsin V antibodies (C,D) or peroxidase-conjugated streptavidin (E), and visualized through enhanced chemiluminescence.

cell types. In some of these cases nuclear localization was the result of exogenous expression of vectors coding for N-terminally truncated cathepsin L in mouse embryonic fibroblasts (Goulet et al., 2004), whereas other examples comprised the spontaneous expression of cathepsin L in mouse ES-cells (Duncan et al., 2008). To further analyze the localization of cysteine cathepsins within HTh74 cells immunofluorescence labeling of cathepsins L and V was performed. These results were consistent with the biochemical data and revealed a predominant localization of cathepsin L to vesicles scattered throughout the cytosol with a preference of accumulation in the peri-nuclear region of HTh74 cells (Figure 7A, green signals). However, almost none of the cathepsin L-specific immunosignals were co-localized with DRAQ5™ in the nuclei of HTh74 cells (Figure 7A). Antibodies directed against the propeptide region of cathepsin V immunoreacted with the nuclei of HTh74 cells (Figure 7B, arrowheads and yellow signals). Most important, and similar to our observations for nuclear cathepsin B variants, the immunoreactions were strongest in cells during telophase or already in cytokinesis, i.e., immunoreactive nuclear cathepsin V variants were most typical for proliferative cells (Figure 7B, arrowheads). Furthermore, antibodies originally raised against cathepsins L and V (Kopitar-Jerala et al., 2001), as well as commercially available antibodies against cathepsin V displayed clear signals over the nuclei of HTh74 cells (Figure 7C,D, arrowheads). The sub-nuclear distribution pattern of cathepsin V was granular throughout the nucleoplasm, excluding the nucleoli (Figure 7E, arrowheads) but with a tendency to a peri-nucleolar localization (Figure 7I, arrowheads). The extra-nucleolar distribution of cathepsin V immunoreactive protein was also visualized by its limited co-localization with PI labeling of the nucleoli (Figure 7F) or with antibodies against coilin (not shown) and by comparison with fibrillarin stainings (Figure 7H). However, the extra-nucleolar, granular staining pattern of nuclear cathepsin

V variants resembled that of HMGB1 (Figure 7G), and partly co-localized with Ki67 at the outer rim of the nucleoli in proliferating cells (Figure 7I, arrowheads).

Discussion

TSH-responsiveness of thyroid cells

In thyroid malignancies, cells might be poorly differentiated such as characteristic for the KTC-1 cell line or they might even have lost most of their epithelial features such as in the anaplastic carcinoma cell lines HTh7 and HTh74. We have shown that HTh74 cells do not express TTF-1, the thyroid-specific transcription factor of ultimate importance for thyrocyte differentiation (Heldin and Westermark, 1991) but here, we show that only HTh74 cells bear TSH-receptor mRNA and that the receptor is functional which is in accordance with earlier studies. Our results led us to conclude on the suitability to use HTh74 cells as a model system for TSH-responsive thyroid carcinoma cells.

Thyroid hormone levels in the blood are regulated through a negative feedback where low thyroxine levels induce the release of TSH from the anterior pituitary which results in an increase in Tg synthesis and release into the follicular lumen. As an early response to TSH stimulation, cysteine cathepsins are retrieved out of endo-lysosomes and are transported to the apical plasma membrane of thyroid epithelial cells for their subsequent secretion into the extracellular follicle lumen under physiological conditions (Brix et al., 2001; Linke et al., 2002a,b). In pathological circumstances, however, it has been suggested that TSH stimulation could promote cathepsin B trafficking to the basolateral plasma membrane domain and its secretion for subsequent ECM degradation in early stages of thyroid malignancies (Kusunoki et al., 1995; Shuja and Murnane, 1996). Therefore, we have analyzed this cysteine cathepsin in a variety of thyroid
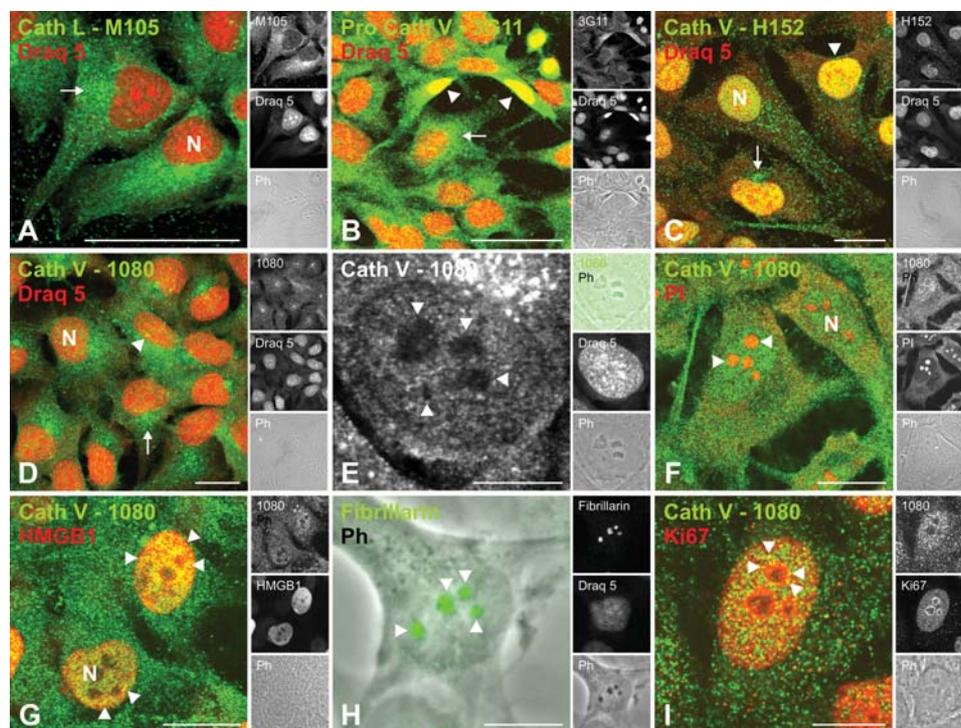
Figure 7   Nuclear localization of cathepsin V in HTh74 cells.
Micrographs of HTh74 cells immunolabeled after PFA fixation and Triton X-100 permeabilization with antibodies raised against cathepsin L (A), procathepsin V (B), cathepsin V (C–G,I), HMGB1 (G), fibrillarin (H), and Ki67 (I). Single-channel fluorescence (right panels, top and middle), merged (A–I) and corresponding phase contrast micrographs (right panels, bottom) are displayed. Nuclei were counter-stained with DRAQ5™ or PI as indicated. Immunolabeling of HTh74 cells revealed vesicular (arrows) and intra-nuclear staining patterns (arrowheads). Note that cathepsin L was absent from the nuclei of HTh74 cells (A), whereas procathepsin V-specific antibodies immunolabeled preferentially the nuclei of cells in telophase (B). Cathepsin V (C–G,I) and HMGB1 (G) were detected within extra-nucleolar regions. Nucleoli were visualized by PI staining (F) or with anti-fibrillarin antibodies (H), and by comparison with dense structures visible within the nuclei of HTh74 cells viewed in phase contrast (Ph). Scale bars correspond to 50 μm in A,B, 20 μm in C,D,F,G, and 10 μm in E,H,I. N denotes nuclei.

carcinoma cell lines with special emphasis on HTh74 cells because of their TSH-responsiveness. TSH stimulation of HTh74 cells, however, did not show any effect on the abundance of pro- or mature forms of cathepsin B. The most striking observation was, however, that an active cathepsin B variant was present in nuclear fractions of TSH-stimulated and non-stimulated HTh74 cells and that it was also immunodetectable in the nuclei of KTC-1, HTh7 and HTh74 cells by morphology.

Nucleus – a new scene of action for cysteine cathepsin variants

An increasing number of publications provide evidence for the nuclear localization of cysteine cathepsin variants and hypothesize proteolytic functions in this subcellular compartment that was previously believed to be offstage for the so-called lysosomal enzymes (Brix, 2005; Brix and Jordans, 2005; Brix et al., 2008). Likewise, the functional spectrum of cysteine cathepsins comprises significantly more than bulk protein degradation (Mort and Buttle, 1997; Turk et al., 2001; Mohamed and Sloane, 2006; Vasiljeva et al., 2007; Brix et al., 2008).

Cysteine cathepsins are proteolytically active in oxidizing and neutral conditions (Gocheva et al., 2006; Vasiljeva and Turk, 2008; Jordans et al., 2009; Turk and Turk, 2009), e.g., in the thyroid follicle lumen where they play a crucial role in thyroid hormone release (Friedrichs et al., 2003). In thyroid cancer, cathepsin B has also been localized to the basolateral plasma membrane and detected at the edge of invasive cells in thyroid carcinoma *in situ* where it is believed to degrade extracellular matrix components (Shuja and Murnane, 1996; Shuja et al., 1999). In this study, we now show that in addition to such extracellular locations and supplementary to the classical vesicular endo-lysosomal localization, a cathepsin B variant is also found in the nuclei of the thyroid carcinoma cell lines KTC-1, HTh7 and HTh74.

Active forms of cathepsin B and V variants in the nucleus of thyroid carcinoma cells

Nuclear variants of cysteine cathepsins were first demonstrated in a seminal study by Goulet and colleagues, further revealing that proteolytic processing of the transcription factor CUX1 by nuclear cathepsin L in mouse embryonic fibro-

blasts led to an earlier S-phase entry (Goulet et al., 2004). This group also showed that the use of alternative start sites is the most plausible explanation for the synthesis of an N-terminally truncated cathepsin L and its subsequent nuclear localization (Goulet et al., 2004). According to the data presented in this study, thyroid carcinoma cells synthesize a proteolytically active variant of cathepsin B that is truncated to reach an apparent molecular mass of approximately 40 kDa and that is sorted to the nucleus of KTC-1, HTh7 and HTh74 cells. N-terminally truncated forms of cathepsin B have been reported before in human malignancies and their translation is believed to be the result of alternative mRNA splicing producing a transcript that codes for a polypeptide lacking the signal peptide and part of the propeptide (Mehtani et al., 1998).

In another example, nuclear cathepsin L and possibly also other family members have been proposed to play a role in development and differentiation of embryonic stem cells owing to the ability to proteolytically process histone H3 tails (Duncan et al., 2008). Hence, a role for nuclear cathepsin L in regulation of transcription was proposed for mouse embryonic stem cells (Duncan et al., 2008). Obviously, the nuclear localization of cysteine cathepsin variants is not exclusive for cathepsins B and L, but other members of the papain-like family of cysteine peptidases seem to be expressed in an N-terminally truncated form too.

In principle, the nuclear cysteine cathepsin variants could cleave a large variety of nuclear substrates owing to the broad substrate specificity of the enzymes. However, as we have shown here by using an *in vitro*-degradation assay, in which histone H1 was identified as a potential target whereas HMGB1 resisted cathepsin B-mediated cleavage for up to 4 h, it is more probably that specific rather than general protein processing occurs, at least within the nuclei of thyroid carcinoma cells. The functional relevance of these findings is still to be determined. It can, however, already now be proposed that the landscape of DNA-associated proteins including nucleosomal histones (Duncan et al., 2008) and linker histone H1 (this study) are probable candidates for proteolytic regulation during cell cycle progression.

Here, we further demonstrate a nuclear localization of a cathepsin V variant in HTh74 cells. In contrast to cathepsins B and V and their variants, cathepsin L displays an exclusive endo-lysosomal localization in the HTh74 thyroid carcinoma cell line as demonstrated through indirect immunofluorescence and subcellular fractionation. It is remarkable that cathepsin L was not expressed as a nuclear variant in these thyroid carcinoma cells, but cathepsin V. Taking into consideration that cathepsin V is not encoded by the mouse genome, we hypothesize that cathepsin V variants in the nuclei of human cells can take part in similar functions as cathepsin L variants acting within the nuclei of mouse cells.

Sub-nuclear localization of cysteine cathepsin variants

Staining patterns of several different cathepsin V-directed mono- and polyclonal antibodies were analyzed and displayed a granulated pattern throughout the nucleus except

for the nucleoli of HTh74 cells. Furthermore, when comparing the staining patterns of the cathepsin V variant with that of coilin, a protein resident in Cajal bodies (Bellini et al., 2000), or with the staining of fibrillarin, a characteristic protein of nucleoli (Ochs et al., 1985), there was no spatial correlation between the cathepsin V variant and these proteins. Rather, a peri-nucleolar localization of cathepsin V could often be detected that was partially overlapping with that of Ki67.

Here we detected exclusively cathepsin V variants but not cathepsin L variants in the nuclei of thyroid carcinoma cells. *In vitro*, it has recently been shown that the inhibition of cathepsin L by stefin B is potentiated in the presence of core histones (Ceru et al., 2010). In analogy to the previous findings, one possible function of the nuclear cathepsin V variant of HTh74 cells would be predicted as to result in proteolytic modifications of histone tails and thereby in regulation of methylation patterns during the onset and progression of thyroid malignancies. From our previous observations *in vitro* (Ong et al., 2007), we indeed hypothesize that an interaction of the cathepsin V variant can occur with other nuclear proteins (Figure 8). Moreover, it is important to note that such interactions could result in conformational changes of chromatin, and that the potential proteolytic activity of a nuclear cathepsin V variant would be adjustable through interaction with, e.g., nuclear serpins in the DNA-rich environment (Ong et al., 2007). Clearly, this proposal needs further investigations aiming at the identification of the interaction part-
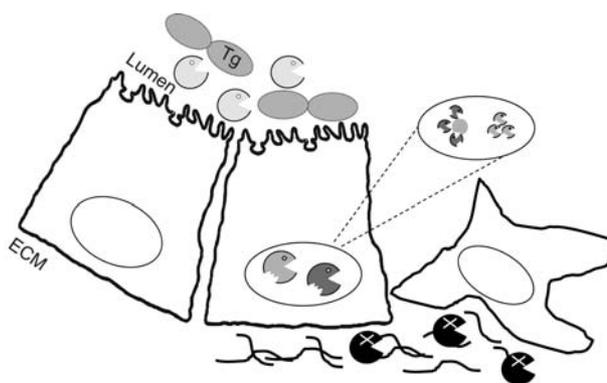

Figure 8 Physiological and pathological localization of cathepsins in thyroid epithelial and carcinoma cells.
Schematic illustration depicting the localization and proposed functions of cysteine peptidases such as cathepsins B and V and their variants in human thyroid cells. Cathepsin B is secreted from thyroid epithelial cells at the apical plasma membrane upon TSH stimulation for extracellular prohormone processing in the thyroid gland under physiological conditions (left). In thyroid cancer, secretion of cathepsin B at the basal pole was observed and is believed to facilitate tumor cell invasion through its contribution to extracellular matrix (ECM) degradation (right). In this study, we describe for the first time the presence of variants of cathepsins B and V in extranucleolar regions of the nuclei of HTh74 cells (middle). We propose a function of nuclear cysteine cathepsin variants in proteolytic processing of DNA-associated and other nuclear proteins which could be important for the malignant characteristics of the cells.

ners of nuclear cysteine cathepsin variants in thyroid carcinoma cells.

Mechanism of nuclear import of cysteine cathepsin variants

The mechanism(s) for the nuclear localization of cysteine cathepsins are still not known, and articles describing nuclear cathepsin variants rarely give any suggestions on the mechanism of nuclear import. Cathepsin B and V do not contain any classical nuclear localization signals (NLS) and the LOCtree and Support Vector Machine systems (Hua and Sun, 2001; Nair and Rost, 2005) predict an extracellular localization of cathepsin B meaning ER entry and transport to the endo-lysosomal compartment. However, truncated cathepsin variants might fold slightly differently (without losing their activity, as shown for cathepsin B variants in Figure 2 and for cathepsin V variants in Figure 6) and thereby exposing so far unknown nuclear localization signals. In an elegant and comprehensive study it was found that several domains exist in the cathepsin B sequence that are believed to allow differential targeting of the molecule to, e.g., nuclei, mitochondria, or to endo-lysosomes (Bestvater et al., 2005). These authors proposed a hierarchy of such different targeting signals depending on their availability. Likewise, by exon skipping a cathepsin B variant is produced that acquires a mitochondrion targeting signal (Muntener et al., 2004).

In addition, protein interactions have been observed between cathepsin V and serpin-6 (Luke et al., 2007; Ong et al., 2007) as well as between cathepsin L and stefin B (Ceru et al., 2010) *in vitro*. Serpins and stefin B are expressed in the cytosol and also localize to the nucleus. Furthermore, an interaction was described between cathepsin B and G0/G1 switch regulatory protein 8 (G0S8; Cell growth-inhibiting gene 31 protein) in a yeast two-hybrid approach (Stelzl et al., 2005). We propose that interactions of cathepsin variants could occur in the cytosol with nuclear proteins before their nuclear import, which would allow the cathepsin variants hitchhiking into the nuclear compartment in complex with these proteins. Such import pathways might add onto the existence of alternative targeting signals in cathepsin variants. Nuclear retention might be through equivalent interaction with nuclear proteins bearing such signals and/or via interaction with DNA.

Perspectives

Once the cathepsin variants enter the nucleus, their subnuclear localization seems to differ considerably. Whereas cathepsin B variants appeared as patches within the nuclear matrix, cathepsin V variants tended to localize to peri-nucleolar regions in that they formed distinct ring-shaped structures around nucleoli as deduced from co-labeling with Ki67. Aberrant nucleoli and numerous peri-nucleolar compartment (PNC) are characteristic for malignant cell phenotypes (Huang et al., 1997). Markers of the PNC are PTB, Raver1 and RNA binding proteins of various kinds. PTB is a key component for PNC structure and is shuttling between the nucleoplasm and the cytosol (Kamath et al., 2001). Constit-

uents of the PNC are believed to be targeted to the juxta-nucleolar region by intrinsic RRMs, RNA recognition motifs, which provide the structural basis for both, interaction with RNA and protein targeting to PNCs. RRMs (Maris et al., 2005) are not present in either cathepsin B or L variants, but partial RRMs consisting of a maximum of four amino acids out of the octa- and hexameric peptide consensus sequences of RRM1 and RRM2, respectively, are present preferentially in the cathepsin V sequence. Hence, we propose that specific mechanisms must exist that localize either of the two cysteine cathepsin variants to specific sub-nuclear locations. Whether cathepsin V has a functional role in peri-nucleolar compartments such as the PNC or whether such a localization is merely a transit point needs to be further analyzed.

Our results allow the interesting possibility that different substrates of truncated cathepsin B and V variants are present in the nuclei of thyroid carcinoma cells. Considering that approximately 700 proteins associate stably with human nucleoli only (Lamond and Earnshaw, 1998), the abundance of potential targets in the entire nucleoplasm makes the search for a specific substrate difficult. However, based on our co-localization studies, we assumed peri-nucleolar proteins as potential targets of nuclear proteases.

In conclusion, we have identified nuclear cysteine cathepsin variants in human thyroid carcinoma cells, and believe that these can promote thyroid tumor progression through a novel mechanism (Figure 8). This notion challenges our view on protease biology and adds another dimension to the mechanisms of action and roles of proteolytic enzymes in physiological and pathological conditions. The novel targets of proteolytic enzymes are suggested to be nuclear components involved in the modulation of DNA structure and in transcriptional regulation. Further studies of this 'new field' of cysteine cathepsins action are of vital importance for a more complete understanding of the mechanisms behind the development and progression of thyroid malignancies and the possibility to develop inhibitors that could be of clinical use.

Materials and methods

Cell culture

The human thyroid carcinoma cell lines KTC-1, HTh7 and HTh74 were grown at 37°C and 5% CO_2 in a moisturized atmosphere. KTC-1 cells were cultured in RPMI-1640 (Biowhittaker, Verviers, Belgium), and HTh7 and HTh74 cells in Eagle's Minimum Essential Medium (Biowhittaker), all supplemented with 10% fetal calf serum (FCS; PerBio, Aalst, Belgium). For analysis of TSH-receptor mRNA, all cells were grown in Coons F-12 medium (Sigma-Aldrich, Taufkirchen, Germany) containing 2.68 mg/ml sodium bicarbonate and supplemented with 5% FCS plus a six-hormone mixture (6H) consisting of 0.166 mg/ml insulin, 2 μg/ml Gly-His-Lys complex, 0.362 μg/ml hydrocortisone, 0.5 μg/ml transferrin, 1 μg/ml somatostatin and 100 μU/ml TSH (final concentrations; all from Sigma-Aldrich). Before TSH stimulation, the cells were cultured in 5H medium, i.e., the medium mentioned above but without FCS and TSH, for 48 h.

RT-PCR

Total RNA was extracted using the RNeasy Mini Extraction Kit (Qiagen, Hilden, Germany). One microgram of RNA from each cell line was used as a template for cDNA synthesis using the Omniscript Reverse Transcription Kit (Qiagen). Each reaction contained 0.5 mM dNTPs, 1 μM random oligonucleotide primers, and 4 U Omniscript Reverse Transcriptase and proceeded at 37°C for 60 min. The cDNA for the human TSH-receptor and β-actin was amplified with the following primers: TSH-receptor sense 5′-TGA AGC TGT ACA ACA ACG GC-3′ and 5′-TCA GTT CCT TCA GGT GCT CC-3′ antisense, as well as β-actin sense 5′-GCT CGT CGT CGA CAA CGG CTC-3′ and antisense 5′-CAA ACA TGA TCT GGG TCA TCT TCT C-3′ (all from Eurofins MWG Operon, Ebersberg, Germany). Each PCR reaction contained 100 pmol primer, 2 U *Taq* DNA polymerase, 1.25 mM MgCl$_2$ and 0.2 mM dNTPs (all from MBI Fermentas, St. Leon-Rot, Germany). TSH-receptor and β-actin cDNA was amplified at annealing temperatures of 57.5°C and 56°C, respectively. The RT-PCR products were separated through 1.5% agarose gel electrophoresis and visualized by inclusion of 0.3% ethidium bromide. A Quick load 100-bp ladder (New England BioLabs, Ipswich, MA, USA) was used as a marker.

Cysteine peptidase tagging with the activity based probe DCG-04

Cells were washed with ice-cold PBS, i.e., 0.9% NaCl, 20 mM NaH$_2$PO$_4$, pH 6.8, and collected in PBS with the use of a cell scraper (Sarstedt, Nümbrecht, Germany). Cell suspensions were centrifuged for 5 min at 130 *g* and cells were lysed in 0.2% Triton X-100 in 200 mM HEPES, pH 7.4, supplemented with 5 μM biotinylated DCG-04 (Greenbaum et al., 2000) for 30 min at 4°C on an end-over-end rotator. Finally, the supernatants were cleared through centrifugation.

Subcellular fractionation

All steps were performed on ice and centrifugations at 4°C. The cells were washed three times with ice-cold PBS before detachment with a cell scraper and collection by centrifugation at 110 *g* for 5 min. The whole cell lysates were prepared by resuspending and incubating the cells in lysis buffer, i.e., 0.2% Triton X-100 in PBS, supplemented with 5 mM EDTA and Protease Inhibitor Cocktail Set III (Merck KGaA, Darmstadt, Germany) for 30 min at 4°C on a head-over-head rotor. The supernatants were cleared through centrifugation at 16 000 *g* for 10 min and stored at -20°C until use. The cells for the nuclear fractions were harvested and resuspended in buffer A, i.e., 10 mM Tris-HCl, 10 mM NaCl, 3 mM MgCl$_2$, 0.5% Nonidet P-40, 10 mM DTT, pH 7.4, and incubated on ice for 5 min followed by centrifugation at 600 *g* for 5 min. The pellets were resuspended in buffer C, i.e., 20 mM HEPES, 25% glycerol (v/v), 500 mM NaCl, 0.2 mM Na$_2$EDTA, 100 mM DTT, pH 7.9, supplemented with protease inhibitors as described above, and incubated for 30 min at 4°C on a head-over-head rotor. The supernatants were cleared and stored as described for the whole cell fraction. For the lysosomal fractions (Brix et al., 1996), the cells were harvested in 100 mM Soerensen phosphate buffer, i.e., 0.067 M KH$_2$PO$_4$ and Na$_2$HPO$_4$, pH 7.2, supplemented with 0.25 M sucrose and 5 mM EDTA. The cell suspensions were homogenized with a Dounce homogenizer (Kontes Co., Vineland, NJ, USA) at 110 rev./min for 5 min on ice. The homogenate was centrifuged at 160 *g* for 5 min and the post-nuclear supernatant subjected to centrifugation at 3000 *g* for 5 min and 10 000 *g* for 20 min. The plasma membrane fractions (Brix et al., 1996) were obtained by overlaying the super-natants of the 10 000 *g* centrifugation step on a two-step cushion of 0.32 and 1.2 M sucrose in Soerensen buffer supplemented with EDTA and centrifuged at 100 000 *g* for 2 h using a swing-out rotor. The pellets of the 10 000 *g* centrifugation represented the lysosomal fractions after lysis for 30 min at 4°C in 0.2% Triton X-100 in PBS, supplemented with 5 mM EDTA and protease inhibitors as above, at pH 5.0, whereas the plasma membrane fractions obtained from the interphase of the sucrose gradient were lysed in the same buffer but at pH 7.4. Lysates were cleared by centrifugation.

In vitro degradation of nuclear proteins

Nuclear fractions (0.2 mg/ml protein) prepared from the HTh74 cell line were incubated with 8 mU cathepsin B from bovine spleen (Sigma-Aldrich) for 0, 1 and 4 h at 37°C under gentle agitation at 300 rev./min. Cathepsin B was not subjected to reducing conditions to approximate nuclear conditions. The proteins were separated through SDS-PAGE as described above but were visualized by silver staining according to the following procedure. The gel was fixed with 40% ethanol and 10% acetic acid followed by incubation with 30% ethanol, 0.1% glutaraldehyde, 0.83 M sodium acetate and 12.6 mM sodium thiosulfate for 30 min. This was followed by incubation with the silver stain solution containing 5.9 mM silver nitrate and 0.01% formaldehyde for 40 min. The gel was incubated with the developer solution containing 0.24 M sodium carbonate and 0.003% formaldehyde until the bands were clearly visible.

SDS-PAGE and immunoblotting

Protein sample concentrations were determined by the Bradford assay (Bradford et al., 1976). The proteins were separated through SDS-PAGE on 12.5% polyacrylamide gels along with a PageRuler Prestained Protein ladder (Fermentas) and transferred to a nitrocellulose membrane by semi-dry blotting. Unspecific binding sites were blocked with 5% milk powder in PBS containing 68 mM NaCl, 63.2 mM Na$_2$HPO$_4$, 11.7 mM NaH$_2$PO$_4$, pH 7.2, supplemented with 0.3% Tween (PBS-T) overnight at 4°C. Incubation with specific antibodies diluted in PBS-T was for 2 h at room temperature with goat anti-mouse cathepsin B (1:1000; Neuromics, Hiddenhausen, Germany), mouse anti-human cathepsin D (IM03; 1:100; Merck KGaA), rabbit anti-human HMGB1 (1:300; Abcam, Cambridge, UK), mouse anti-human cathepsin V (MAB1080; 1:250; R&D Systems, Minneapolis, USA), mouse anti-human cathepsin L clone 33/1 (1:1000; EW) and mouse anti-human histone H1 (1:500; Leinco Technologies, Saint Louis, MO, USA) was followed by incubation with horseradish peroxidase-conjugated secondary antibodies (Southern Biotech, Birmingham, AL, USA) for 1 h at room temperature. Incubation with the peroxidase substrate was followed by visualization through enhanced chemiluminescence on XPosure films (both from ThermoScientific/Pierce, Bonn, Germany). DCG04-labeled proteins were visualized by incubation of the blots for 1 h at room temperature with peroxidase-conjugated streptavidin (Dianova, Hamburg, Germany).

Indirect immunofluorescence

Cells used for indirect immunofluorescence experiments were cultured on cover slips in 6-well plates. After washing with calcium- and magnesium-free PBS (CMF-PBS), i.e., 0.15 M NaCl, 2.7 mM KCl, 1.5 mM NaH$_2$PO4, 8.1 mM Na$_2$HPO4, pH 7.4, the cells were fixed with 4% paraformaldehyde in 200 mM HEPES, pH 7.4, for 30 min at room temperature. Permeabilization after washing was in 0.2% Triton X-100 in CMF-PBS for 5 min at room temperature. For blocking, 3% bovine serum albumin (BSA; Carl Roth GmbH,

Karlsruhe, Germany) in CMF-PBS was used for 1 h at 37°C. Cells were incubated with primary antibodies diluted in 0.1% BSA in CMF-PBS overnight at 4°C. Specific antibodies were anti-mouse cathepsin B (1:200; Neuromics), mouse anti-human cathepsin L clone M105 (1:25) (Kopitar-Jerala et al., 2001), mouse anti-human procathepsin V clone 3G11 (1:100; EW), mouse anti-human cathepsin L and V clone H152 (1:25) (Kopitar-Jerala et al., 2001), mouse anti-human cathepsin V MAB1080 (1:50; R&D Systems), mouse anti-human fibrillarin (1:25; Abcam), rabbit anti-HMGB1 (1:500; Abcam) and rabbit anti-Ki67 (1:50; Abcam). After washing, Alexa 488-conjugated secondary antibodies (1:200; Molecular Probes, Karlsruhe, Germany) were incubated with the cells for 1 h at 37°C together with 5 mM DRAQ5™ (Biostatus Ltd., Shepshed Leicestershire, UK) or 2 μg/ml propidium iodide (Carl Roth GmbH) which were used as nuclear counter-stains. After washing with CMF-PBS and de-ionized water, the cover slips were mounted with embedding medium consisting of 33% glycerol, 14% Mowiol in 200 mM Tris-HCl, pH 8.5 (Hoechst, Frankfurt, Germany) on microscopic slides. The immunofluorescence samples were viewed with a confocal laser scanning microscope (LSM 510 Meta; Carl Zeiss Jena GmbH, Jena, Germany) and analyzed with the LSM 510 software, Release 3.2 (Carl Zeiss Jena GmbH).

Acknowledgments

References

Bellini, M. (2000). Coilin, more than a molecular marker of the cajal (coiled) body. Bioessays 22, 861–867.

Berquin, I.M., Cao, L., Fong, D., and Sloane, B.F. (1995). Identification of two new exons and multiple transcription start points in the 5′-untranslated region of the human cathepsin-B-encoding gene. Gene 159, 143–149.

Bestvater, F., Dallner, C., and Spiess, E. (2005). The C-terminal subunit of artificially truncated human cathepsin B mediates its nuclear targeting and contributes to cell viability. BMC Cell Biol. 6, 16.

Bradford, M.M. (1976). A rapid and sensitive method for the quantitation of microgram quantities of protein utilizing the principle of protein-dye binding. Anal. Biochem. 72, 248–254.

Brix, K. (2005). Lysosomal proteases: revival of the sleeping beauty. In: Lysosomes, P. Saftig, ed. (Georgetown, USA: Landes Bioscience/Eurekah.com, Springer Science + Business Media, Inc.), pp. 50–59.

Brix, K. and Jordans, S. (2005). Watching proteases in action. Nat. Chem. Biol. 1, 186–187.

Brix, K., Lemansky, P., and Herzog, V. (1996). Evidence for extracellularly acting cathepsins mediating thyroid hormone liberation in thyroid epithelial cells. Endocrinology 137, 1963–1974.

Brix, K., Linke, M., Tepel, C., and Herzog, V. (2001). Cysteine proteinases mediate extracellular prohormone processing in the thyroid. Biol. Chem. 382, 717–725.

Brix, K., Dunkhorst, A., Mayer, K., and Jordans, S. (2008). Cysteine cathepsins: cellular roadmap to different functions. Biochimie 90, 194–207.

Bromme, D., Li, Z., Barnes, M., and Mehler, E. (1999). Human cathepsin V functional expression, tissue distribution, electrostatic surface potential, enzymatic characterization, and chromosomal localization. Biochemistry 38, 2377–2385.

Bulynko, Y.A., Hsing, L.C., Mason, R.W., Tremethick, D.J., and Grigoryev, S.A. (2006). Cathepsin L stabilizes the histone modification landscape on the Y chromosome and pericentromeric heterochromatin. Mol. Cell Biol. 26, 4172–4184.

Buth, H., Luigi Buttigieg, P., Ostafe, R., Rehders, M., Dannenmann, S.R., Schaschke, N., Stark, H.J., Boukamp, P., and Brix, K. (2007). Cathepsin B is essential for regeneration of scratch-wounded normal human epidermal keratinocytes. Eur. J. Cell Biol. 86, 747–761.

Ceru, S., Konjar, S., Maher, K., Repnik, U., Krizaj, I., Bencina, M., Renko, M., Nepveu, A., Zerovnik, E., Turk, B., et al. (2010). Stefin B interacts with histones and cathepsin L in the nucleus. J. Biol. Chem. 285, 10078–10086.

Duncan, E.M., Muratore-Schroeder, T.L., Cook, R.G., Garcia, B.A., Shabanowitz, J., Hunt, D.F., and Allis, C.D. (2008). Cathepsin L proteolytically processes histone H3 during mouse embryonic stem cell differentiation. Cell 135, 284–294.

Fonovic, M. and Bogyo, M. (2008). Activity-based probes as a tool for functional proteomic analysis of proteases. Expert. Rev. Proteomics 5, 721–730.

Friedrichs, B., Tepel, C., Reinheckel, T., Deussing, J., von Figura, K., Herzog, V., Peters, C., Saftig, P., and Brix, K. (2003). Thyroid functions of mouse cathepsins B, K, and L. J. Clin. Invest. 111, 1733–1745.

Gocheva, V., Zeng, W., Ke, D., Klimstra, D., Reinheckel, T., Peters, C., Hanahan, D., and Joyce, J.A. (2006). Distinct roles for cysteine cathepsin genes in multistage tumorigenesis. Genes Dev. 20, 543–556.

Gong, Q., Chan, S.J., Bajkowski, A.S., Steiner, D.F., and Frankfater, A. (1993). Characterization of the cathepsin B gene and multiple mRNAs in human tissues: evidence for alternative splicing of cathepsin B pre-mRNA. DNA Cell Biol. 12, 299–309.

Goulet, B., Baruch, A., Moon, N.S., Poirier, M., Sansregret, L.L., Erickson, A., Bogyo, M., and Nepveu, A. (2004). A cathepsin L isoform that is devoid of a signal peptide localizes to the nucleus in S phase and processes the CDP/Cux transcription factor. Mol. Cell 14, 207–219.

Goulet, B., Truscott, M., and Nepveu, A. (2006). A novel proteolytically processed CDP/Cux isoform of 90 kDa is generated by cathepsin L. Biol. Chem. 387, 1285–1293.

Goulet, B., Sansregret, L., Leduy, L., Bogyo, M., Weber, E., Chauhan, S.S., and Nepveu, A. (2007). Increased expression and activity of nuclear cathepsin L in cancer cells suggests a novel mechanism of cell transformation. Mol. Cancer Res. 5, 899–907.

Greenbaum, D., Medzihradszky, K.F., Burlingame, A., and Bogyo, M. (2000). Epoxide electrophiles as activity-dependent cysteine protease profiling and discovery tools. Chem. Biol. 7, 569–581.

Heldin, N.E. and Westermark, B. (1991). The molecular biology of the human anaplastic thyroid carcinoma cell. Thyroidology 3, 127–131.

Hua, S. and Sun, Z. (2001). Support vector machine approach for protein subcellular localization prediction. Bioinformatics 17, 721–728.

Huang, S., Deerinck, T.J., Ellisman, M.H., and Spector, D.L. (1997). The dynamic organization of the perinucleolar compartment in the cell nucleus. J. Cell Biol. 137, 965–974.

Irving, J.A., Shushanov, S.S., Pike, R.N., Popova, E.Y., Bromme, D., Coetzer, T.H., Bottomley, S.P., Boulynko, I.A., Grigoryev, S.A., and Whisstock, J.C. (2002). Inhibitory activity of a heterochromatin-associated serpin (MENT) against papain-like cys-

teine proteinases affects chromatin structure and blocks cell proliferation. J. Biol. Chem. *277*, 13192–13201.

Jordans, S., Jenko-Kokalj, S., Kuhl, N.M., Tedelind, S., Sendt, W., Bromme, D., Turk, D., and Brix, K. (2009). Monitoring compartment-specific substrate cleavage by cathepsins B, K, L, and S at physiological pH and redox conditions. BMC Biochem. *10*, 23.

Joyce, J.A., Baruch, A., Chehade, K., Meyer-Morse, N., Giraudo, E., Tsai, F.Y., Greenbaum, D.C., Hager, J.H., Bogyo, M., and Hanahan, D. (2004). Cathepsin cysteine proteases are effectors of invasive growth and angiogenesis during multistage tumorigenesis. Cancer Cell *5*, 443–453.

Kamath, R.V., Leary, D.J., and Huang, S. (2001). Nucleocytoplasmic shuttling of polypyrimidine tract-binding protein is uncoupled from RNA export. Mol. Biol. Cell *12*, 3808–3820.

Kopitar-Jerala, N., Bevec, T., Barlic-Maganja, D., Gubensek, F., and Turk, V. (2001). Anti-cathepsin L monoclonal antibodies that distinguish cathepsin L from cathepsin V. Biol. Chem. *382*, 867–870.

Kusunoki, T., Nishida, S., Nakano, T., Funasaka, K., Kimoto, S., Murata, K., and Tomura, T. (1995). Study on cathepsin B activity in human thyroid tumors. Auris Nasus Larynx *22*, 43–48.

Lamond, A.I. and Earnshaw, W.C. (1998). Structure and function in the nucleus. Science *280*, 547–553.

Lemansky, P., Brix, K., and Herzog, V. (1998). Iodination of mature cathepsin D in thyrocytes as an indicator for its transport to the cell surface. Eur. J. Cell Biol. *76*, 53–62.

Linke, M., Herzog, V., and Brix, K. (2002a). Trafficking of lysosomal cathepsin B-green fluorescent protein to the surface of thyroid epithelial cells involves the endosomal/lysosomal compartment. J. Cell Sci. *115*, 4877–4889.

Linke, M., Jordans, S., Mach, L., Herzog, V., and Brix, K. (2002b). Thyroid stimulating hormone upregulates secretion of cathepsin B from thyroid epithelial cells. Biol. Chem. *383*, 773–784.

Ludwig, T., Munier-Lehmann, H., Bauer, U., Hollinshead, M., Ovitt, C., Lobel, P., and Hoflack, B. (1994). Differential sorting of lysosomal enzymes in mannose 6-phosphate receptor-deficient fibroblasts. EMBO J. *13*, 3430–3437.

Luke, C.J., Pak, S.C., Askew, Y.S., Naviglia, T.L., Askew, D.J., Nobar, S.M., Vetica, A.C., Long, O.S., Watkins, S.C., Stolz, D.B., et al. (2007). An intracellular serpin regulates necrosis by inhibiting the induction and sequelae of lysosomal injury. Cell *130*, 1108–1119.

Mach, L., Mort, J.S., and Glossl, J. (1994). Maturation of human procathepsin B. Proenzyme activation and proteolytic processing of the precursor to the mature proteinase, *in vitro*, are primarily unimolecular processes. J. Biol. Chem. *269*, 13030–13035.

Maris, C., Dominguez, C., and Allain, F.H. (2005). The RNA recognition motif, a plastic RNA-binding platform to regulate posttranscriptional gene expression. FEBS J. *272*, 2118–2131.

Mayer, K., Vreemann, A., Qu, H., and Brix, K. (2009). Release of endo-lysosomal cathepsins B, D, and L from IEC6 cells in a cell culture model mimicking intestinal manipulation. Biol. Chem. *390*, 471–480.

Mehtani, S., Gong, Q., Panella, J., Subbiah, S., Peffley, D.M., and Frankfater, A. (1998). *In vivo* expression of an alternatively spliced human tumor message that encodes a truncated form of cathepsin B. Subcellular distribution of the truncated enzyme in COS cells. J. Biol. Chem. *273*, 13236–13244.

Mohamed, M.M. and Sloane, B.F. (2006). Cysteine cathepsins: multifunctional enzymes in cancer. Nat. Rev. Cancer *6*, 764–775.

Mort, J.S. and Buttle, D.J. (1997). Cathepsin B. Int. J. Biochem. Cell Biol. *29*, 715–720.

Muntener, K., Zwicky, R., Csucs, G., Rohrer, J., and Baici, A. (2004). Exon skipping of cathepsin B: mitochondrial targeting of a lysosomal peptidase provokes cell death. J. Biol. Chem. *279*, 41012–41017.

Nair, R. and Rost, B. (2005). Mimicking cellular sorting improves prediction of subcellular localization. J. Mol. Biol. *348*, 85–100.

Ochs, R.L., Lischwe, M.A., Spohn, W.H., and Busch, H. (1985). Fibrillarin: a new protein of the nucleolus identified by autoimmune sera. Biol. Cell *54*, 123–133.

Ong, P.C., McGowan, S., Pearce, M.C., Irving, J.A., Kan, W.T., Grigoryev, S.A., Turk, B., Silverman, G.A., Brix, K., Bottomley, S.P., et al. (2007). DNA accelerates the inhibition of human cathepsin V by serpins. J. Biol. Chem. *282*, 36980–36986.

Reinheckel, T., Deussing, J., Roth, W., and Peters, C. (2001). Towards specific functions of lysosomal cysteine peptidases: phenotypes of mice deficient for cathepsin B or cathepsin L. Biol. Chem. *382*, 735–741.

Riese, R.J. and Chapman, H.A. (2000). Cathepsins and compartmentalization in antigen presentation. Curr. Opin. Immunol. *12*, 107–113.

Shuja, S. and Murnane, M.J. (1996). Marked increases in cathepsin B and L activities distinguish papillary carcinoma of the thyroid from normal thyroid or thyroid with non-neoplastic disease. Int. J. Cancer *66*, 420–426.

Shuja, S., Cai, J., Iacobuzio-Donahue, C., Zacks, J., Beazley, R.M., Kasznica, J.M., O'Hara, C.J., Heimann, R., and Murnane, M.J. (1999). Cathepsin B activity and protein levels in thyroid carcinoma, Graves' disease, and multinodular goiters. Thyroid *9*, 569–577.

Sloane, B.F. and Honn, K.V. (1984). Cysteine proteinases and metastasis. Cancer Metastasis Rev. *3*, 249–263.

Stelzl, U., Worm, U., Lalowski, M., Haenig, C., Brembeck, F.H., Goehler, H., Stroedicke, M., Zenkner, M., Schoenherr, A., Koeppen, S., et al. (2005). A human protein-protein interaction network: a resource for annotating the proteome. Cell *122*, 957–968.

Sullivan, S., Tosetto, M., Kevans, D., Coss, A., Wang, L., O'Donoghue, D., Hyland, J., Sheahan, K., Mulcahy, H., and O'Sullivan, J. (2009). Localization of nuclear cathepsin L and its association with disease progression and poor outcome in colorectal cancer. Int. J. Cancer *125*, 54–61.

Turk, B. and Turk, V. (2009). Lysosomes as 'suicide bags' in cell death: myth or reality? J. Biol. Chem. *284*, 21783–21787.

Turk, B., Turk, D., and Turk, V. (2000). Lysosomal cysteine proteases: more than scavengers. Biochim. Biophys. Acta *1477*, 98–111.

Turk, V., Turk, B., and Turk, D. (2001). Lysosomal cysteine proteases: facts and opportunities. EMBO J. *20*, 4629–4633.

Turk, V., Kos, J., and Turk, B. (2004). Cysteine cathepsins (proteases) – on the main stage of cancer? Cancer Cell *5*, 409–410.

Vasiljeva, O. and Turk, B. (2008). Dual contrasting roles of cysteine cathepsins in cancer progression: apoptosis versus tumour invasion. Biochimie *90*, 380–386.

Vasiljeva, O., Reinheckel, T., Peters, C., Turk, D., Turk, V., and Turk, B. (2007). Emerging roles of cysteine cathepsins in disease and their potential as drug targets. Curr. Pharm. Des. *13*, 387–403.